

# Magnetism and structure at a vacancy in graphene

M. W. C. Dharma-wardana<sup>1,\*</sup> and Marek Z. Zgierski<sup>2,†</sup>

<sup>1</sup> Institute for Microstructural Sciences, National Research Council of Canada

<sup>2</sup> Stacie Institute of Molecular Sciences, National Research Council of Canada, Ottawa, Canada K1A 0R6

(Dated: November 8, 2018)

The electronic structure, bonding and magnetism in graphene containing vacancies are studied using density-functional methods. The single-vacancy graphene ground state is spin polarized and structurally flat. The unpolarized state is non planar only for finite segments. Systems containing periodic arrays of vacancies displays magnetic transitions and metal-insulator transitions.

PACS numbers: PACS Numbers: 71.10.Lp,75.70.Ak,73.22-f

*Introduction*– Graphene is a two-dimensional (2D) sheet of carbon atoms forming a honey-comb lattice, with promising novel technologies and new physics[1, 2]. These include applications based on carbon nanotubes[3, 4] which are topologically equivalent to folded graphene ribbons. Graphene nanoribbons have delocalized states only in one dimension, with conductive and localized edge states. The localized states appear as “flat bands” near the Fermi energy, within tight-binding models which do not treat the lattice relaxation of the edge atoms[5, 6].

When lattice relaxation is included via first-principles calculations, with the dangling bonds saturated with H atoms[8], the electronic structure is found to depend specifically on the ribbon width and the relaxed edge structure. Band gaps are found to appear at the Fermi energy. The role of edges in graphene nanoribbons in producing magnetic ground states has also been studied using such methods[9].

At finite temperatures, entropy as well as the 2D structure of graphene favours disorder. These lead to a quasi-3D wavy conformation[10, 11]. Many authors have also used vacancy or defect models[12] to include disorder effects in the graphene system. However, our calculations[13] for vacancies and also N-substituted defects in graphene showed that the energy costs of such defects are large enough to prevent natural occurrences of such lattice defects, thus differing from metals or semiconductors. Hence in ref. 13 we concluded that the graphene samples used in initial quantum Hall-effect studies were *good samples* basically free of vacancies. However, vacancies and defects can be artificially introduced, and used to control the energy and spin states near the Fermi energy. The vacancies may be positioned lithographically to generate graphene containing a periodic array of vacancies. Such arrays are metastable, and can be annealed to give various forms of *tattered graphene*. The tattering occurs because two second-neighbour vacancies are found to coalesce into a more stable divacancy, which form a sink for other second-neighbour vacancies. More distant vacancies simply distort the  $\sigma$ -bonding skeleton and stabilize themselves. Individual vacancies carry a spin polarization, and provide

a new type of qubit for quantum computational devices. The variations in spin polarization and band-gaps with the vacancy concentration set the stage for magnetic and metal-insulator transitions. Hence here we study an infinite graphene sheet with periodically distributed vacancies using a plane-wave density-function theory (DFT) approach based on the Vienna ab-initio simulation code (VASP[14]). We also study finite segments of graphene, with real-space DFT-calculations using Gaussian basis sets (Gaussian-98 code[15]). The finite graphene studied here have zig-zag edges terminated with hydrogen atoms.

The finite graphenes with a vacancy give a planar spin-polarized ground state, while the unpolarized state is slightly higher in energy ( $\sim 200$  meV) and show a non-planar, saddle-like structure (see Fig. 1).

The creation of the vacancy removes 4 electrons, and at the same time releases three  $sp^2$  electrons (dangling bonds) and a  $\pi$ -electron. The  $sp^2$ -type electrons are associated with the atoms marked “a, b, c” in Fig. 1. The  $\pi$ -electron is common to these three sites. The system distorts or spin polarizes to accommodate these dangling bonds and the free charges (4 per vacancy). The vacancy is surrounded by three pentagons. The *tri-pentagonal* structure has one pentagon smaller than the other two, enabling a singlet interaction between the atoms “b” and “c” which are closely positioned, compared to the pairs “a, b” and “a, c” of the other two pentagons. The atom “a” in the unpolarized structure (UPS), juts upwards (two views of the structure are given in Fig. 1), while the atoms marked “b, c” dip downwards. This distortion disconnects the  $\pi$ -electron generated by the vacancy from the rest of the 2D electron network. The atom “a” of the UPS carries a lone-pair singlet of electrons, making the total structure unpolarized. The sheet around the vacancy acquires a saddle-like distortion. The two bonds associated with ‘X’, and the atom ‘a’ defining the edge of the vacancy are shortened ( $\sim 1.39\text{\AA}$ ) compared to the normal  $1.42\text{\AA}$  bond length in graphene.

The lower-energy (ground) state is the planar spin-polarized structure (PSPS). Two views of it are given in Fig. 1. The stabilization energy for this system (44 hexagons with a zig-zag edge saturated with H atoms),

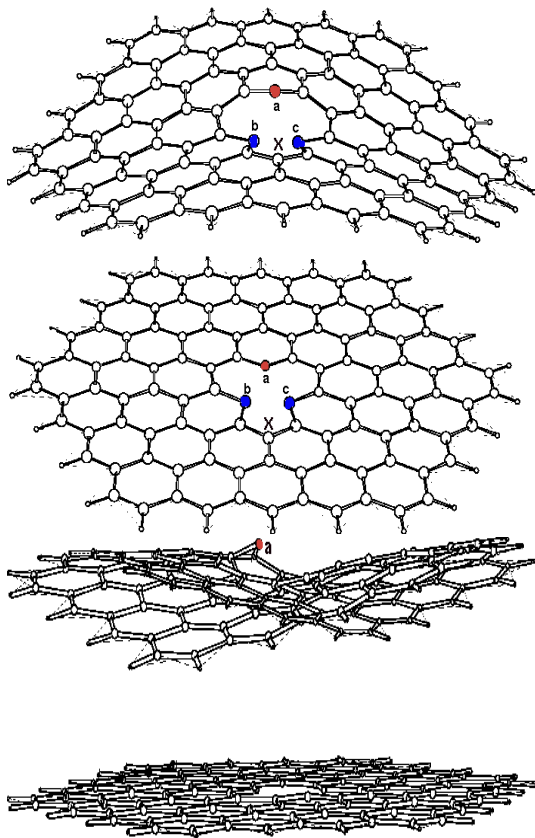


FIG. 1: (Color online) Relaxation of a finite sheet (44 hexagons) of graphene containing a vacancy. The carbon atoms marked “a, b, c” were bound to the C atom removed to form the vacancy. The bent structure shows the non-planar graphene sheet where the four electrons released by the vacancy are accommodated to form a spin-unpolarized structure. The ground state is planar and spin-polarized. Two views of it are shown. The atoms marked ‘b’, ‘c’ (in blue) are close enough in both structures to form a singlet interaction. The atom ‘a’ (in red) juts upwards in the unpolarized structure and carries an unpaired electron. The atoms ‘X’ and ‘a’ have two short bonds in the pentagons.

compared to the unpolarized state is 217 meV, i.e., comparable to room-temperature energies. This result is obtained with a Gaussian-98 DFT calculation using the Becke-Lee-Yang-Parr (B3LYP) exchange-correlation metafunctional[16] within a Gaussian (6-31G\*, see Ref. [17] for definitions) basis set. The short distance between atoms “b, c” enables the two  $sp^2$  dangling bonds to form a singlet. The atom “a” now carries one  $sp^2$ -electron spin, unlike in the UPS where two (i.e., a lone-pair singlet) electrons are localized. Here again the bonds at “a” and “X” defining the edge of the vacancy are short. The  $\pi$  electron released from the vacancy delocalizes into the 2D network around the vacancy in the PSPS. In fig. 2 we show the distribution of excess charge projected on the  $x$ - $y$  plane of the graphene sheet.

On comparing the panels (a) and (b) of Fig. 2 it is

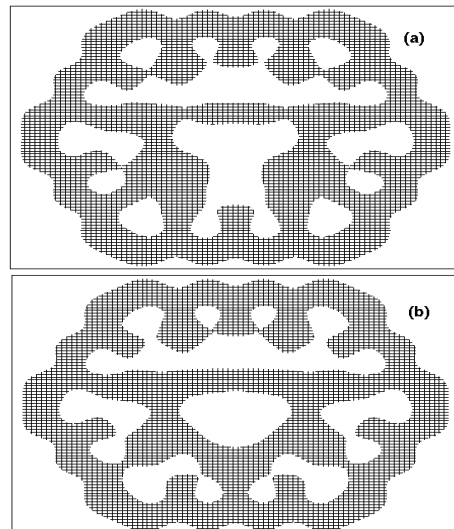


FIG. 2: The distribution of excess charge density (hatched areas) in the 2D plane of the graphene sheet around a vacancy, for the structure shown in Fig. 1, for the spin-unpolarized (a) and polarized (b) case.

clear that the charge depletion caused by the unpolarized structure is significantly larger than in the polarized structure of panel (b). In the PSPS, (b), the  $\pi$  electron released from the formation of the vacancy re-distributes itself among the three pentagons. This simplified discussion of the  $\pi$ -electron charge at the vacancy has to be extended to allow the  $\pi$ -electron to spread in the full 2D-network bounded by the edge-C atoms. The edge defines a “zig-zag” termination (saturated with hydrogen atoms in this calculation). A plot of the Mullikan spin charge ( $n_\alpha - n_\beta$ ), obtained from a spin-polarized DFT calculation (using Gaussian-98) is shown in Fig. 3 for the structure of Fig. 1. The total spin of the structure is consistent with a triplet state made up of the  $sp^2$  electron on the carbon atom ‘a’ and the  $\pi$ -electron. It is also noted that some of the spin-polarization resides at the graphene-edge seen in the depth of the figure. This suggests that the finite-graphene segment studied here is not large enough for the vacancy to be isolated from the edge effects. The electronic density of states (DOS) for these are also shown in the bottom panel. The DOS of the unpolarized state was divided by 2 to compare with the polarized states, and a Lorentzian broadening of 0.3 eV has been applied. The DOS shows substantial filling around  $E_F$ , due to the localized states at  $E_F$  created by the formation of the vacancy.

The finite-graphenes necessarily limit the  $\pi$ - electrons to a localized region. The boundary conditions imposed on the wavefunctions do not allow true extended states. This difficulty is overcome in calculations where periodic boundary conditions in the  $x$ - $y$  plane are used. We consider simulation cells with  $N_a \times N_b$  graphene unit cells, each cell containing two carbon atoms, with a lat-

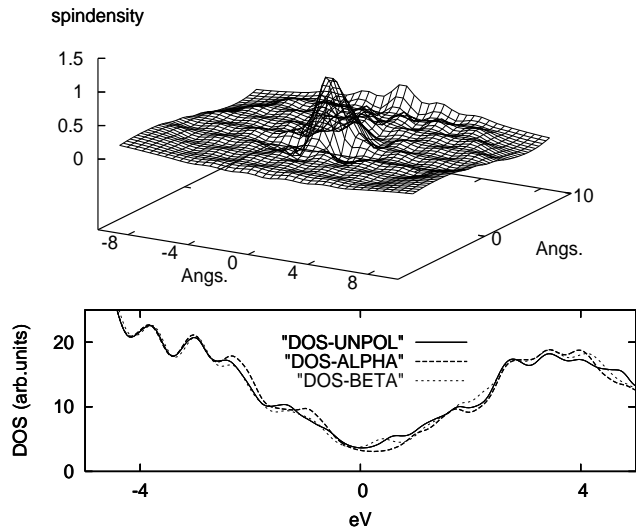


FIG. 3: The top panel gives the spin density ( $n_\alpha - n_\beta$ ) where  $n_\sigma$  is the spin-dependent Mullikan charge on each C atom of the planar structure. The structure of the flat graphene piece is given in Fig. 1. The bottom panel shows the Electronic density of states (DOS) for the unpolarized system (bent structure) and for the flat, polarized ground state. The  $E_F$  is set to zero and calculated with a Lorentzian broadening of 0.3 eV.

tice parameter  $a_0 = 2.47\text{\AA}$ . and a C-C bond length of  $1.42\text{\AA}$  in unperturbed graphene. Calculations are mostly for  $N_a = N_b$  for  $N_a = 2, 3, 4$ , and 6, corresponding to  $N = 2N_a^2$  of 8, 18, 32 and 72 carbon atom in the graphene simulation cell (SC). These calculations use the VASP[14] plane-wave code (clearly, no terminating-H atoms are needed). Projected augmented-wave (PAW) pseudopotentials[14] have been used for Carbon. The C pseudopotential is well established and was used in several graphene-type calculations (e.g., Ref. 11, 13, 18). Removal of one C atom from the test structures gives vacancy concentrations  $x_v$  of  $1/8$ ,  $1/18$ ,  $1/32$ , and  $1/72$ . The finite-graphene piece studied using Gaussian-98 calculations contained 112 C atoms less one due to the vacancy. Of these, 46 were edge atoms. Thus, the finite graphene is possibly analogous to an extended system with a vacancy concentration  $x_v$  of  $\sim 1/66$  if the edge effect is negligible in the above finite-system. Similarly, the periodic simulation cell with 36 unit cells and 72 C atoms,  $x_v = 1/72$  is the most “isolated” vacancy studied here, the periodic image being six unit cells away. The systems with  $x_v \geq 1/32$  increasingly contain vacancy-vacancy interactions, since the periodic repetitions of the SC would place vacancies at 4, 3, and 2 units of  $a_0$  from each other.

When vacancies are introduced into graphene, the large stresses are relieved by some neighbours (C-atoms near the vacancy) moving towards the vacancy, while

others move away. The distortion persists to at least the third set of neighbours, and generates a bond-length distribution varying from about  $1.37\text{\AA}$  to  $1.45\text{\AA}$ . If several vacancies are present in the system, the energy minimization enables some vacancies to migrate and form divacancies. Thus the initial periodic structures can be “annealed” to give structures which are (at least) at local energy minima. Here we report results for systems with only one vacancy per simulation cell. The structure optimization involves (i) optimization of all atomic positions in a given simulation cell with  $N_a \times N_b$  unit cells and optimization of the cell parameter  $a_0$ , (ii) repeating spin-density functional calculations till convergence of energies, and negligible Hellman-Feynman forces (to less than  $0.001\text{ eV/\AA}$ ) are obtained. Details of integration grids, simulation cells etc., are similar to those discussed in previous work[11, 13]. Unlike in our results for finite graphene, no out-of-plane distortions were found in the periodic systems studied here, irrespective of the spin-polarization. The calculations for periodic systems also reproduce a tri-pentagonal vacancy, similar to the vacancy in finite graphenes. Both systems are shown in Fig. 1.

In Fig. 4 we summarize our results for the magnetism and stabilization of graphene sheets containing periodic realizations of vacancies. The unpolarized planar system is the ground state for systems with vacancies in excess of  $x_v \sim 0.06$ . At these higher vacancy levels, the atoms move sufficiently close to each other and singlet pairing becomes possible. At lower  $x_v$ , the situation seems to be similar to the finite-graphene system where one of the  $sp^2$  electrons remains unpaired, localized at the atomic site ‘a’. The uncoupled  $\pi$ -electron becomes a part of the 2D electron fluid since the C-skeleton remains planar. The intriguing result obtained from the VASP calculation is that the net magnetization (i.e.,  $n_\alpha - n_\beta$ ) accumulated within the simulation cell can take a fractional value in the spin-polarized case. This result remains robust when tested by increasing the size of the  $k$ -integration grids, and varying other technical parameters of the calculation. One possibility suggests some sort of spin and charge fractionation. The shortened pair of bonds at the atom ‘a’, and at the atom ‘X’ suggests that additional electron localization occurs around them. The  $\pi$ -electron released in forming the vacancy remains near the vacancy, shared among the three pentagons defined by the atoms ‘a’, ‘b’ and ‘c’ of the vacancy (Fig. 1). However, a  $1/3$  spin-charge seems to be available for alignment with (or against) the spin already localized on the atom ‘a’. The calculations attempt to examine such possibilities using explicit spin-density functional calculations which reliably predicts spin ground states. It is found that the spin localizes around the vacancy and aligns ferromagnetically for  $x_v < 1/20$ , (given the maximum spin of 1.333) and antiferromagnetically for  $1/20 < x_v < 1/16$ , i.e., a magnetization of 0.66). Thus the low vacancy regime

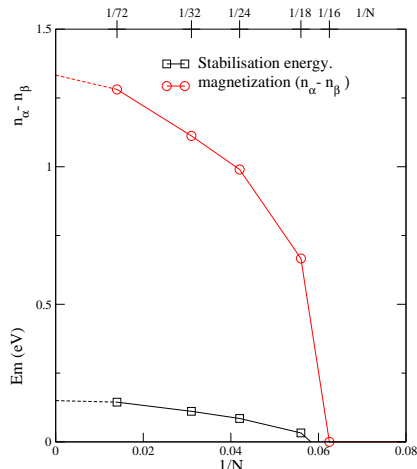


FIG. 4: (Color online) The stabilization energy  $E_{pol} - E_{unp}$ , and the spin polarization of the graphene vacancy, with one vacancy per simulation cell (containing  $N$  lattice sites), and periodically repeated. The polarized and unpolarized structures are planar. The unpolarized planar ground state is stable for  $x_v > \sim 0.06$ .

gives a net spin polarization  $n_z = (n_\alpha - n_\beta)$  such that  $1.333 < n_z < 0.666$ , while the intermediate regime shows  $0.666 < n_z < 0$ . The high vacancy regime is unpolarized. The present calculation cannot sharply pin down the actual transitions or rigorously establish these suggestions.

The electronic DOS indicated in Fig. 3 for finite graphene shows significant density of states near  $E_F$ . The situation is similar for infinite graphene with periodic vacancies. The high vacancy (unpolarized) systems have an energy gap. However, depending on the location of  $E_F$  within the band structure, even within a rigid band model we see that the system may or may not be a metal, depending on the vacancy concentration  $x_v$ . This issue needs a fuller discussion in a separate study.

The fore-going considerations suggest that the interaction of the 2D electrons containing the  $\pi$ -electron released from the vacancy, with the localized  $sp^2$ -electron spin on the atom 'a' has features of the Kondo problem, as well as fractional-charge/spin physics. Investigation of such matters would be best carried out within a more analytical approach, complemented by the results of computational approaches similar to the present study.

In conclusion, we have demonstrated, using finite as well as periodic structure calculations, that the ground state of a graphene sheet (held in free space at zero temperature) containing an isolated vacancy is spin polarized. When the concentration of vacancies (realized as a periodic array) exceeds  $\sim 0.06$ , the unpolarized structure

becomes the ground state. All calculations using periodic boundary conditions lead to planar structures. Only the finite-graphene pieces which are unpolarized become distorted.

\* Electronic address: chandre.dharma-wardana@nrc-cnrc.gc.ca

† Email address: marek.zgierski@nrc-cnrc.gc.ca

- [1] A.K. Geim, and K. S. Novoselov, Nature Materials **6**, 183 (2007)
- [2] Y. B. Zhang, Y.-W. Tan, H. L. Stormer, P. Kim, Nature (London), **438**, 201 (2005)
- [3] R. Saito, M. Fujita, G. Dresselhaus and M. S. Dresselhaus, Phys. Rev. B **46** 1804 (1992)
- [4] N. Tit and M. W. C. Dharma-wardana, Europhys. Lett., **62**, 405 (2003) J. Gonzalez, Phys. Rev. Lett. **88**, 76403 (2002).
- [5] M. Fujita, K. Wakabayashi, K. Nakada, K. Kusakabe, J. Phys. Soc. Jpn. **65**, 1920 (1996); M. Ezawa, Phys. Rev. B **73**, 045432 (2006)
- [6] L. Brey and H. A. Fertig, Phys. Rev. B **73** 235411 (2006);
- [7] A. Yamashiro, Y. Shimo, K. Harigaya, and K. Wakabayashi, Phys. Rev. B **68**, 193410 (2003); J. M. Pereira Jr., V. Mlinar, F. M. Peeters, and P. Vasilopoulos, Phys. Rev. B **74**, 045424 (2006)
- [8] Li Yang, Cheol-Hwan Park, Young-Woo Son, Marvin L. Cohen, and Steven G. Louie, Phys. Rev. Lett. **99**, 186801 (2007)
- [9] Oded Hod, Vernica Barone, and Gustavo E. Scuseria, Phys. Rev. B **77**, 035411 (2008); L. Pisani, J. A. Chan, B. Montanari, and N. M. Harrison, Phys. Rev. B **75**, 064418 (2007)
- [10] J. C. Meyer, A. K. Geim, M. I. Katsnelson, K. S. Novoselov, T. J. Booth, and S. Roth, <http://arxiv.org/pdf/cond-mat/0701379>; J. Martin, N. Akerman, G. Ulbricht, T. Lohmann, J. H. Smet, K. von Klitzing, A. Yacoby, *ibid*, arXiv:0705.2180
- [11] M. W. C. Dharma-wardana, J. Phys.: Condens. Matter vol. 19 (2007) 386228
- [12] N. M. R. Peres, F. Guinea and A. H. Castro Neto, Phys. Rev. B **72**, 174406 (2005); **73**, 125411 (2006); T. O. Wehling, A. V. Balatsky, M. I. Katsnelson, A. I. Lichtenstein, K. Scharnberg, R. Wiesendanger, *cond-mat/0609503*
- [13] M. W. C. Dharma-wardana, Phys. Rev. B vol. 75, 075427 (2007)
- [14] Regarding the VASP code, see G. Kress, J. Furthmüller and J. Hafner, <http://cms.mpi.univie.ac.at/vasp/>
- [15] *Gaussian 98*, Revision A.9, M. J. Frisch et al, Gaussian Inc., Pittsburgh, PA (1998).
- [16] see: A.D. Becke, J. Chem. Phys., **98**, 5648 (1993); C. Lee, W. Yang and R.G. Parr, Phys. Rev. B, **37**, 785 (1988).
- [17] The 6-31G\* basis and related acronyms are explained in ref. [16]
- [18] Yuchen Ma, A. S. Foster, A. V. Krasheninnikov, and R. M. Nieminen, Phys. Rev. B **72**, 205416 (2005); B. I. Dolan and J. C. Boettger, J. Phys. B: At. Mol. Phys. **29**, 4907 (1996);

